Analysis of Distribution and Intraparticle Diffusion of a Fluorescent Dye in Mesoporous Silica Gel by Confocal Fluorescence Microspectroscopy

Tatsumi Sato and Kiyoharu Nakatani[†]

Division of Chemistry, Faculty of Pure and Applied Sciences, University of Tsukuba, 1-1-1 Tennoudai, Tsukuba, Ibaraki 305–8571, Japan

A micrometer-sized spherical silica gel microparticle (pore diameter, ~7 nm) was injected into an aqueous rhodamine 6G solution using microcapillary manipulation-injection technique, and the dye distribution in the single microparticle was measured as the fluorescence depth profile by confocal fluorescence microspectroscopy. The fluorescence depth profile was simulated by the convolution and deconvolution methods to correct the contribution of the spatial resolution of the experimental system. The dye homogeneously or heterogeneously distributed in the microparticle at the adsorption equilibrium, dependent on the type of silica gel. The intraparticle diffusion coefficient of the dye distributed homogeneously in the silica gel was analyzed by the simulations of the time dependence of the fluorescence depth profile based on the external and intraparticle diffusion model. The results indicated that the intraparticle diffusion of the dye in the silica gel is governed by the pore diffusion.

Introduction

Porous materials have been used as separation materials and catalyst supports in solution. High functionality of the porous material is caused by a high specific surface area, interaction between a solute and adsorption sites of the pore walls, effective mass transfer of the solute in the pores, and so forth.[1-3] Quantitative analyses of adsorption/desorption and reaction at solid/liquid interfaces, diffusion in the pore solution (pore diffusion) and at the pore walls (surface diffusion), and mass transfer of the solute between the material surface and the bulk solution phase (external mass transfer) in porous material/ solution systems have been demonstrated by chromatographic analysis for a large number of microparticles,[4,5] microspectroscopic analysis for individual microparticles,[6-11] and so on.[12-14] Nonetheless, detailed consideration will be required for analysis of individual elementary processes because various processes are included in the porous material/solution systems. Furthermore, the chemical and physical processes in the pores are influenced by the pore size and the pore distribution. If the pore size and the pore distribution of a porous material at a domain are different from those at another domain, the quantitative and mechanistic analyses are complicated.

We previously reported the intraparticle diffusion of rhodamine 6G (Rh6G) in silica gel/water systems using an absorption microspectroscopy method combined with a single microparticle injection technique.[7,8,15] Based on the absorption microspectroscopy, however, we could only determine the total

concentration of the dye in the single microparticle, so the intraparticle diffusion was indirectly analyzed as the particle size dependence of the diffusion coefficient. Recently, we have developed the confocal fluorescence microspectroscopy method combined with the single microparticle injection technique.[16,17] Using the technique, time dependence of coumarin 102 distribution as a depth profile of the fluorescence intensity in a single ODS-silica gel microparticle in an aqueous solution could be directly observed at the time greater than ~1 min. In the system, the concentration gradient of coumarin 102 between the particle surface and the particle interior was not observed, so the intraparticle diffusion of the dye was expected to be very fast.[16]

In this report, we reexamined the intraparticle diffusion of Rh6G in the single silica gel microparticle/water system using the confocal fluorescence microspectroscopy method combined with the single microparticle injection technique. By the confocal fluorescence microspectroscopy with three-dimensional spatial resolution, detailed information on distribution of the fluorescent dye in the microparticle could be obtained. We show the quantitative analysis procedures of the fluorescent dye distribution in the microparticle, and discuss physical properties of silica gel prepared by two different methods and intraparticle diffusion of the dye in the mesoporous silica gel/solution system.

Experimental

Silica Gel 60 (spherical silica gel) (SG-I; Kanto Chemical Co.: particle radius (r_p), 20 – 50 μm; surface area (A_s), 700 m²/g; pore diameter (d_p), 6.5 nm; pore volume, 1.15 cm³/g), DM 50-60 A Silica Gel (spherical silica gel) (SG-II; AGC Si-Tech. Co.: r_p, 20 – 30 μm; A_s, 609 m²/g; d_p, 6.6 nm; pore volume,

---

[†] To whom correspondence should be addressed.
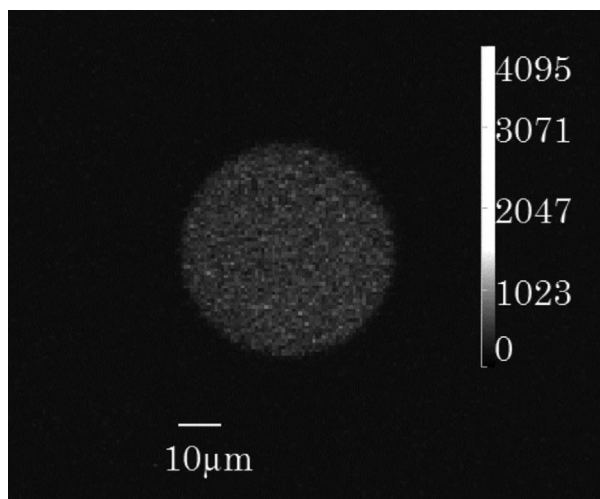E-mail: nakatani@chem.tsukuba.ac.jp

Fig. 1   Confocal fluorescence microscopic image of rhodamine 6G at the adsorption equilibrium in a lateral (xy axes) area including the center of a single SG-I microparticle (r_p = 24.4 μm) injected into an aqueous rhodamine 6G solution.

Fig. 2   Time dependence of fluorescence depth profile of rhodamine 6G in a single (a) SG-I (r_p = 24.4 μm) or (b) SG-II microparticle (r_p = 24.8 μm) injected into an aqueous rhodamine 6G solution. The solid curves represent the simulations by (a) Eqs. (1) and (2), and (b) Eqs. (1) and (3) using $F_0 = 0.74$. The dashed curves represent the simulations by Eqs. (1), (2) and (4) – (10) using $D_p = 5 \times 10^{-9}$ cm²/s.

1.01 cm³/g), rhodamine 6G (Rh6G; Aldrich, 99%), and 2-propanol (Kishida, 99.8%) were used without further purification. Water was used after deionization and distillation (Yamato Scientific, Auto Still WG203). SG-I or SG-II was immersed overnight in water at room temperature.

For uptake rate measurements of Rh6G by confocal fluorescence microspectroscopy, several SG-I or SG-II microparticles in water were transferred to an aqueous HCl solution (0.01 mol/dm³) containing 2-propanol (0, 0.1, 0.2 or 0.5 mol/dm³) and left for over 1 h. Then, the single microparticle was injected into an aqueous Rh6G (1.0×10^{-7}, 3.0×10^{-7}, 5.0×10^{-7} or 1.9×10^{-6} mol/dm³) and HCl (0.01 mol/dm³) solution containing 2-propanol (0, 0.1, 0.2 or 0.5 mol/dm³) using a microcapillary manipulation-injection system (Narishige, MN-151/IM-16). As previously reported in detail, three-dimensional spatially resolved fluorescence measurements of single microparticles were demonstrated by a confocal fluorescence microscope (Olympus, FV 1000-D).[16] Fluorescence (525 – 625 nm) of Rh6G from the single microparticle was measured at 25.0 ± 0.5°C using a CW diode laser (473 nm, 0.45 mW), a confocal aperture of 100 μm diameter, a water-immersion objective lens (Olympus, UPLSAPO 60XW), and a temperature controller (Tokai Hit, MATS-555RO).

For adsorption isotherm measurements, several silica gel microparticles in the 0.01 mol/dm³ HCl solution were dispersed into an aqueous Rh6G (1.0×10^{-6} – 1.1×10^{-5} mol/dm³) and HCl (0.01 mol/dm³) solution containing 2-propanol (0, 0.1, 0.2 or 0.5 mol/dm³) by the microcapillary manipulation-injection method, and left for over 1 h at 25°C. The Rh6G concentrations in the single microparticle ($C_{p,eq}$) and the aqueous solution at the adsorption equilibrium were determined by absorption microspectroscopy and conventional absorption spectroscopy, respectively.[7]

Results and Discussion

Confocal fluorescence microspectroscopy of single silica gel microparticles

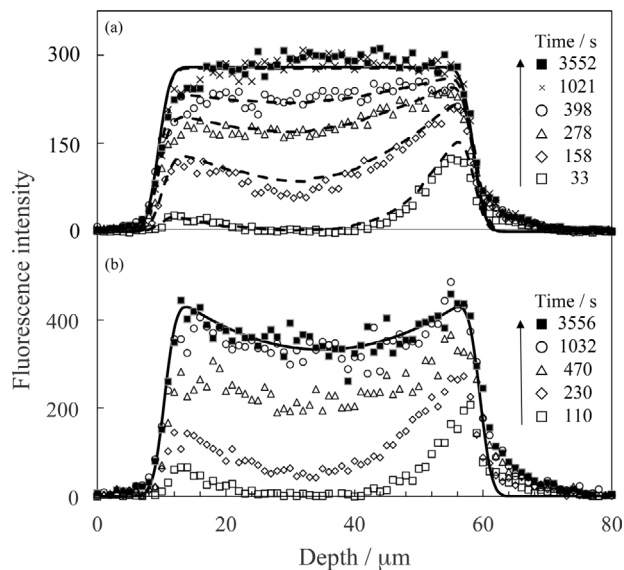SG-I and SG-II are transmissive microparticles, so Rh6G in

the silica gel microparticle in water is excited by visible light and the fluorescence image of Rh6G can be directly measured using a confocal fluorescence microscope (Fig. 1). The fluorescence intensity of a circle with 4.1 μm radius as a lateral (xy axes) area from lower part to upper part of the microparticle along the central axis was analyzed as a fluorescence depth (longitudinal (z) axis) profile.[16] Figure 2 shows the time (t) course of a fluorescence depth profile of Rh6G in a single microparticle injected into an aqueous solution. When a microparticle was just injected into the solution, the t was defined as 0. The microparticle sank in water on a glass plate without Brownian motion of the particle. Cationic Rh6G adsorbs onto the pore wall of silica gel by ion-exchange with H⁺ of a silanol group and distributes into the microparticle interior. Fluorescence intensity of Rh6G from the solution phase was negligibly small in the present system. In the microparticle, the fluorescence intensity depended on the depth and t, and was saturated at prolonged t (adsorption equilibrium), indicating that the uptake rate of Rh6G is governed by intraparticle mass transfer of Rh6G. The asymmetric depth profile will be attributed to the restricted external diffusion of Rh6G at the lower side of the microparticle. It is noteworthy that the shape of the fluorescence depth profile of Rh6G in SG-II (Fig. 2b) is different from that in SG-I at the adsorption equilibrium (Fig. 2a).

The shape of the fluorescence depth profile of Rh6G in SG-I at the adsorption equilibrium is analogous to that of coumarin 102 in ODS-silica gel in water.[16] Although the fluorescence intensity near the spherical surface of the microparticle is slightly smaller than that in the particle interior, that is expected to be due to the spatial resolution of the confocal fluorescence microscope. We suppose that Rh6G homogeneously distributes in SG-I, independent of the depth. On the other hand, the amount of Rh6G molecules near the spherical microparticle surface is greater than that near the microparticle center in SG-II.
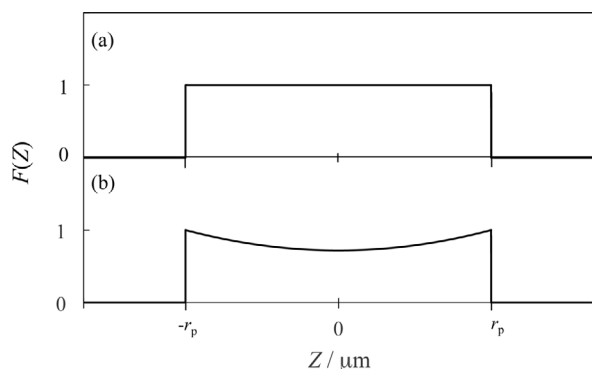
Fig. 3 $F(Z)$ used as a correct depth profile function at the adsorption equilibrium in the (a) SG-I or (b) SG-II system.

Fig. 4   Schematic illustration of a single microparticle/water system for the simulations of the time dependence of fluorescence depth profile.

Simulation of Rh6G distribution in silica gel at adsorption equilibrium

The fluorescence intensity at a position observed by the confocal fluorescence microscope contains the fluorescence not only at the position but also at the adjacent positions, depending on spatial resolution of the confocal microscope. The spatial resolution is influenced by the objective lens magnification, the confocal aperture size, refractive indices of the microparticle and water, and so forth. We simulated the fluorescence depth profiles under the present experimental conditions.

We assume that the fluorescence quantum yield of Rh6G is independent of the depth of the microparticle. Spread of fluorescence from a position is assumed to be given by Eq. (1) as a Gaussian function ($E(z)$),[18]

$$E(z) = \exp\{-A(z - Z)^2\} \tag{1}$$

where Z and A are the point of fluorescence source and the parameter corresponding to the fluorescence spread, respectively. A correct depth profile function ($F(Z)$) of Rh6G distributed in a spherical microparticle at the adsorption equilibrium is assumed to be a rectangular function in the SG-I system (Eq. (2)) (Fig. 3a). The origin of the Z axis is the microparticle center.

$$F(Z) = 0 \text{ (at } Z < -r_p,\ r_p < Z) \text{ or } 1 \text{ (at } -r_p \leq Z \leq r_p) \tag{2}$$

We convoluted $E(z)$ and $F(Z)$ over the microparticle region under the conditions of $\Delta z = \Delta Z = 1$ μm. The depth profile calculated by the method was normalized to compare with that observed in the SG-I system and then A was determined to be 0.807 by the method of least squares (Fig. 2a). We consider that the present calculation is successfully demonstrated because Rh6G homogeneously distributes in SG-I.

For SG-II, $F(Z)$ is assumed to be approximated by a quadratic function given by Eq. (3) (Fig. 3b).

$$F(Z) = 0 \text{ (at } Z < -r_p,\ r_p < Z) \text{ or}$$
$$\{(1 - F_0)/r_p^2\}Z^2 + F_0 \text{ (at } -r_p \leq Z \leq r_p) \tag{3}$$

where F_0 is the constant. The physical properties such as a refractive index of SG-II will be analogous to those of SG-I. Using $E(z)$ as $A = 0.807$, F_0 of $F(Z)$ was determined by the deconvolution method. The fluorescence depth profile calculated by the method was normalized to compare with that observed in the SG-II system and was plotted using $F_0 = 0.74$ (Fig. 2b). The result indicates that the amount of Rh6G molecules near the microparticle center is 0.7 times that near the
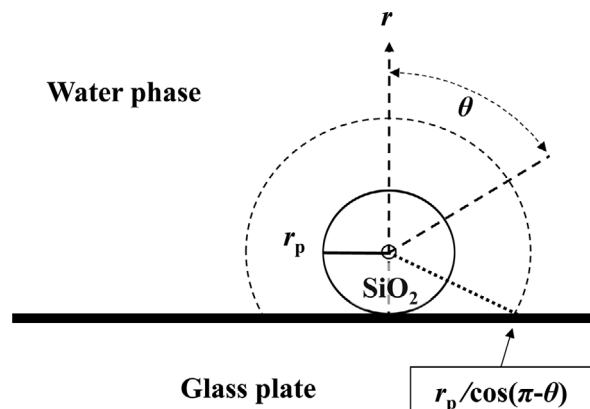
microparticle surface in SG-II. SG-I was prepared by a general sol-gel method. On the other hand, SG-II was produced by a sol-gel method in a water-in-oil emulsion system. In SG-II, the decrease in number of pores and/or decrease in d_p near the microparticle center will be observed.

Simulation of Rh6G diffusion in the SG-I/water system

Dissociation of silanol groups of silica gel in water scarcely proceeds at pH 2 and ionic strength in water is 0.01 mol/dm³, so contribution of migration of the cationic Rh6G to the uptake rate into the microparticle will be neglected. Therefore, the uptake rate of Rh6G will be limited by the intraparticle and external diffusions. In previous reports, the intraparticle diffusion of Rh6G in silica gel was analyzed by a spherical diffusion equation based on the Fick's second law as the external diffusion is assumed to be very fast.[7,8,15] In the present model, both the external diffusion including the restricted external diffusion at the lower side of the microparticle and the intraparticle diffusion of Rh6G are considered. The t dependence of a concentration profile of Rh6G ($C_i(r, \theta, t)$, i = p or w) in the microparticle ($C_p(r, \theta, t)$) or water ($C_w(r, \theta, t)$) is given by the diffusion equation (Eq. (4)).

$$\partial C_i(r, \theta, t)/\partial t = D_i\{(1/r^2)\partial/\partial r(r^2\partial/\partial r) + 1/(r^2\sin\theta)\partial/\partial\theta(\sin\theta\partial/\partial\theta)\}C_i(r, \theta, t) \tag{4}$$

where r is the radially-directed spatial coordinate and θ is the elevation angle (Fig. 4). D_i (i = p or w) is the diffusion coefficient of Rh6G in the microparticle (D_p) or bulk water phase ($D_w = 4.0 \times 10^{-6}$ cm²/s).[19] The initial conditions are given by

$$C_p(r, \theta, 0) = 0 \qquad \text{(at } 0 \leq r \leq r_p) \tag{5}$$

$$C_w(r, \theta, 0) = C_{w0} \qquad \text{(at } r_p \leq r) \tag{6}$$

where C_{w0} is the Rh6G concentration in the bulk water phase. In the present system, C_{w0} can be assumed to be equal to the Rh6G concentration before the single microparticle injection because the volume of the solution (5 cm³) is much larger than that of the single microparticle (~10⁻⁸ cm³). The boundary conditions are given by

$$\partial C_p(0, \theta, t)/\partial r = 0 \tag{7}$$

Table 1　Langmuir isotherm parameters of Rh6G in the SG-I/water system in the absence and presence of 2-propanol

2-Propanol concentration/ mol dm^{-3}	$K_L C_{p,L}$	$C_{p,L}$/ 10^{-4} mol dm^{-3}	K_L/ 10^5 dm^3 mol^{-1}
0	168 ± 8	6.5 ± 0.7	2.6 ± 0.3
0.1	55.3 ± 2.5	7.8 ± 1.6	0.70 ± 0.15
0.2	33.5 ± 1.1	5.5 ± 0.8	0.61 ± 0.09
0.5	17.4 ± 1.1	6.1 ± 4.7	0.29 ± 0.22

$$\partial C_p(r, 0, t)/\partial \theta = \partial C_p(r, \pi, t)/\partial \theta = 0 \qquad (8)$$

$$\partial C_p(r_p, \theta, t)/\partial r = K_L C_{p,L} C_w(r_p, \theta, t)/(1 + K_L C_w(r_p, \theta, t)) \qquad (9)$$

$$\partial C_w(r, \theta, t)/\partial r = \partial C_w(r, \theta, t)/\partial \theta = 0$$
$$(\text{at } r_p/\cos(\pi - \theta) < r, \pi/2 < \theta) \qquad (10)$$

where K_L and $C_{p,L}$ are the Langmuir isotherm constant and the saturated amount of Rh6G adsorbed in silica gel, respectively, determined from the slope ($K_L^{-1}C_{p,L}^{-1}$) and the intercept ($C_{p,L}^{-1}$) of the $C_{p,eq}^{-1}$ vs. C_{w0}^{-1} plot (Langmuir isotherm). Thus, the t dependence of the concentration profile was simulated by a finite form for various D_p values under the conditions of $\Delta t = 1$ ms, $\Delta r = 1$ µm, and $\Delta \theta = \pi/18$. Then, the Rh6G concentration depth profile was obtained from the simulation of the external and intraparticle diffusions, and was convoluted by the above method using Eqs. (1) and (2) as $A = 0.807$. The observed fluorescence depth profiles were fitted by the simulations (Fig. 2a) and the D_p value was determined to be 5×10^{-9} cm^2/s in the absence of 2-propanol using the observed K_L and $C_{p,L}$ values (Table 1). Previously, as the external diffusion in water is assumed to be much faster than the intraparticle diffusion, D_p of Rh6G in SG-I using the absorption microspectroscopy was roughly estimated to be $(4 - 5) \times 10^{-9}$ cm^2/s at 0.01 mol/dm^3 HCl,[7] whose value agreed almost with that determined by the present method.

Figure 5 shows the observed and calculated fluorescence depth profiles of Rh6G in the presence of 2-propanol. The time required to the adsorption equilibrium decreased with the increasing 2-propanol concentration in the water phase. K_L decreased with the increasing 2-propanol concentration while $C_{p,L}$ was independent of the 2-propanol concentration (Table 1). Adsorption of Rh6G is expected to be suppressed owing to a decrease in permittivity in the water phase by the addition of 2-propanol. By the simulations using Eqs. (1), (2), and (4) – (10), D_p was determined to be 1.5×10^{-8} cm^2/s for 0.1 mol/dm^3 2-propanol (Fig. 5a). For 0.5 mol/dm^3 2-propanol, the observed fluorescence depth profile was independent of t, indicating that the adsorption equilibrium of Rh6G is reached within 116 s (Fig. 5b). D_p was estimated to be greater than 5×10^{-8} cm^2/s. We consider that D_p smaller than $\sim 5 \times 10^{-8}$ cm^2/s can be determined by the present technique.

Pore and surface diffusion of Rh6G in the SG-I/water system

According to the pore and surface diffusion model proposed by Ruthven et al., D_p is given by the equation: $D_p = D_w H/\{\tau_w(1 + R)\} + D_s R/\{\tau_s(1 + R)\}$,[3,20] where D_s and H are the surface diffusion coefficient and the hindrance parameter dependent on the molecular diameter of the solute (a) and d_p, respectively. τ_w or τ_s is the tortuosity for the pore or surface diffusion, respectively, and was reported to be 1.5 – 2.3 for silica gel.[21] R is the distribution coefficient of Rh6G between the
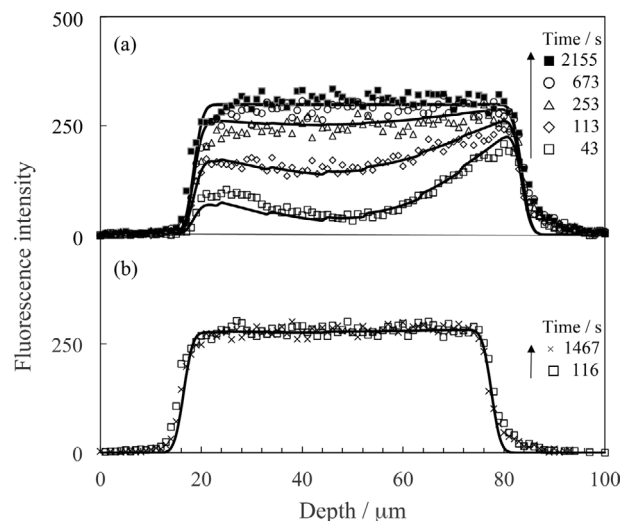

Fig. 5　Time dependence of fluorescence depth profile of rhodamine 6G in a single SG-I microparticle injected into an aqueous rhodamine 6G solution containing 2-propanol of (a) 0.1 mol/dm^3 ($r_p = 32.7$ µm) or (b) 0.5 mol/dm^3 ($r_p = 30.2$ µm). The solid curves represent the simulations by Eqs. (1), (2) and (4) – (10) using $D_p = $ (a) 1.5×10^{-8} or (b) 5×10^{-8} cm^2/s.
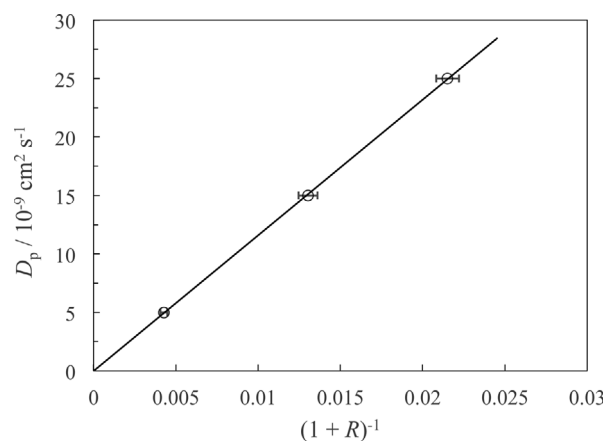

Fig. 6　Relationship between D_p and R for 0, 0.1 and 0.2 mol/dm^3 2-propanol in the SG-I system.

particle and the solution phase, and is estimated as $R = (K_L C_{p,L}/\varepsilon_p) - 1$ (Table 1),[21] where ε_p is the porosity of silica gel (0.72).[21] The first and second terms of the right side of the equation (D_p) correspond to the pore and surface diffusion terms, respectively. In the present system, the surface diffusion term is approximated to be D_s/τ_s due to $R \gg 1$.

Figure 6 shows the observed D_p vs. $(1 + R)^{-1}$ plot for 0, 0.1 and 0.2 mol/dm^3 2-propanol. D_p was directly proportional to $(1 + R)^{-1}$. D_s is estimated to be $< \sim 10^{-10}$ cm^2/s from the intercept of the plot. From the slope of the plot, H is determined to be 0.44 for $\tau_w = \tau_s = 1.5$ (0.58 for $\tau_w = \tau_s = 2$) using $D_w = 4.0 \times 10^{-6}$ cm^2/s.[19] Based on the Renkin equation: $H = \{1 - (a/d_p)\}^2 \times \{1 - 2.10(a/d_p) + 2.09(a/d_p)^3 - 0.95(a/d_p)^5\}$,[22] H is estimated to be 0.42 using $a = 1.2$ nm and $d_p = 6.5$ nm,[15] and almost agrees with the observed H. Therefore, the intraparticle diffusion is governed by the pore diffusion, and the surface diffusion is neglected in the Rh6G-SG-I/water system. Previously, we discussed the pore and surface diffusion of Rh6G in the SG-I/
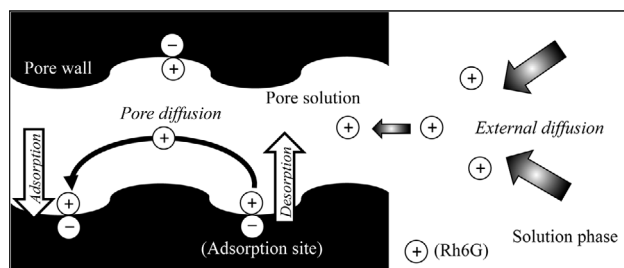
Fig. 7   Schematic illustration of intraparticle diffusion of rhodamine 6G in the SG-I/water system.

water system from the ion-strength dependence of D_p in the absence of 2-propanol by the absorption microspectroscopy.[15] The present result is consistent with the result for the ion-strength dependence of D_p.

The occupied area of an adsorbed Rh6G molecule (S) in the SG-I system will be estimated by $S = A_s/[N_A C_{p,L}/\{\rho_s(1 - \varepsilon_p)\}]$, where ρ_s and N_A are the particle density of silica gel (2.2 g/cm³)[21] and the Avogadro constant, respectively. Using $A_s = 700$ m²/g and $C_{p,L} = 6.5 \times 10^{-4}$ mol/dm³ (Table 1), S was calculated to be 1.1×10^{-15} m², whose value corresponds to the circle area with a radius of 19 nm. The distance between the adjacent adsorption sites (38 nm) on the pore walls is much larger than $a = 1.2$ nm for Rh6G. Therefore, Rh6G adsorbed at a site on the pore walls should be desorbed to diffuse in the pores so that contribution of the surface diffusion will be neglected in the intraparticle diffusion (Fig. 7). In ODS-silica gel/solution systems, intraparticle diffusion of a solute has been reported to be governed by the surface diffusion.[20,23,24] In the ODS-silica gel system, the distance between the adjacent octadecylsilyl groups as the adsorption sites is short due to the long alkyl group, so the surface diffusion will effectively proceed.

Conclusions

The distribution and the intraparticle diffusion of Rh6G in the porous silica gel microparticle in the aqueous solution were elucidated by the confocal fluorescence microspectroscopy combined with the single microparticle injection technique. The fluorescence depth profile of the dye in the microparticle was quantitatively analyzed by the digital simulations. The heterogeneous dye distribution was observed in the SG-II system, different from the homogeneous distribution in the SG-I system. It was suggested that the intraparticle diffusion of the dye in the SG-I system is limited by the pore diffusion. We consider that the present approach is indispensable for detailed mechanistic analysis on mass transfer and chemical reactions proceeding in the porous microparticles.

References

 1. D. M. Ruthven, "*Principles of Adsorption and Adsorption Processes*", **1984**, Wiley, New York.
 2. N. Wu, M. A. Hubbe, O. J. Rojas, and S. Park, *BioResources*, **2009**, *4*, 1222.
 3. D. M. Ruthven, *Chem. Eng. Sci.*, **2004**, *59*, 4531.
 4. K. Miyabe and M. Suzuki, *AIChE J.*, **1995**, *41*, 548.
 5. R. Bujalski and F. F. Cantwell, *J. Chromatogr. A*, **2004**, *1048*, 173.
 6. H.-B. Kim, M. Hayashi, K. Nakatani, N. Kitamura, K. Sasaki, J. Hotta, and H. Masuhara, *Anal. Chem.*, **1996**, *68*, 409.
 7. K. Nakatani and T. Sekine, *Langmuir*, **2000**, *16*, 9256.
 8. T. Sekine and K. Nakatani, *Langmuir*, **2002**, *18*, 694.
 9. K. Nakatani, M. Miyanaga, and Y. Kawasaki, *Anal. Sci.*, **2011**, *27*, 1253.
10. N. Kameta, H. Minamikawa, Y. Someya, H. Yui, M. Masuda, and T. Shimizu, *Chem. Eur. J.*, **2010**, *16*, 4217.
11. H. Xu, S. Nagasaka, N. Kameta, M. Masuda, T. Ito, and D. A. Higgins, *Phys. Chem. Chem. Phys.*, **2016**, *18*, 16766.
12. M. D. Ludes, S. R. Anthony, and M. J. Wirth, *Anal. Chem.*, **2003**, *75*, 3073.
13. A. Yamaguchi, M. M. Mekawy, Y. Chen, S. Suzuki, K. Morita, and N. Teramae, *J. Phys. Chem. B*, **2008**, *112*, 2024.
14. F. Roncaroli and M. A. Blesa, *J. Colloid Interface Sci.*, **2011**, *356*, 227.
15. T. Sekine and K. Nakatani, *Chem. Lett.*, **2004**, *33*, 600.
16. K. Nakatani and E. Matsuta, *Anal. Sci.*, **2015**, *31*, 557.
17. K. Nakatani, E. Matsuta, and Y. Kawasaki, *Bunseki Kagaku*, **2016**, *65*, 145.
18. A. Small and S. Stahlheber, *Nat. Methods*, **2014**, *11*, 267.
19. P.-O. Gendron, F. Avaltroni, and K. J. Wilkinson, *J. Fluoresc.*, **2008**, *18*, 1093.
20. R. Bujalski and F. F. Cantwell, *Anal. Chem.*, **2006**, *78*, 1593.
21. R. Bujalski and F. F. Cantwell, *Langmuir*, **2001**, *17*, 7710.
22. W. M. Deen, *AIChE J.*, **1987**, *33*, 1409.
23. K. Miyabe and G. Guiochon, *Anal. Chem.*, **2000**, *72*, 1475.
24. K. Miyabe, S. Sotoura, and G. Guiochon, *J. Chromatogr. A*, **2001**, *919*, 231.